Experimental and theoretical study of the ground-state $M1$ transition in Ag-like tungsten

Z. Fei,[1,2] R. Zhao,[1,2] Z. Shi,[1,2] J. Xiao,[1,2] M. Qiu,[1,2] J. Grumer,[3] M. Andersson,[1,2] T. Brage,[3] R. Hutton,[1,2,*] and Y. Zou[1,2,†]

[1]*The Key Lab of Applied Ion Beam Physics, Ministry of Education, China*

[2]*Shanghai EBIT Laboratory, Modern Physics Institute, Fudan University, Shanghai, China*

[3]*Division of Mathematical Physics, Department of Physics, Lund University, Sweden*

(Received 13 August 2012; published 3 December 2012)

We present an experimental and theoretical study of the $^2F_{5/2} \rightarrow {}^2F_{7/2}$ $M1$ transition in Ag-like W (W^{27+}). The experiments employed the Shanghai permanent magnet electron beam ion trap, which has been developed especially for assisting spectroscopic diagnostics of edge plasmas for magnetic fusion devices. The theoretical value was obtained using the GRASP2K set of computer codes and included a comprehensive correlation study. The experimental $M1$ wavelength was measured as 3377.43 ± 0.26 Å (3378.43 Å vacuum wavelength), whereas the calculated wavelength is in good agreement at 3381.80 Å. This good agreement shows the importance of fully understanding the electron correlation effects to predict the energy of the fine structure even in this, for tungsten, relatively simple case.

DOI: 10.1103/PhysRevA.86.062501 PACS number(s): 32.30.Jc, 32.70.Fw, 31.15.aj

I. INTRODUCTION

Tungsten, because of its excellent thermomechanical properties and its very low erosion under various physical and chemical conditions, is considered as a strong candidate for the plasma facing material for future fusion devices. But as a heavy element, it exhibits very high radiation power, so a small fraction of W atoms in a fusion plasma could lead to dramatic effects on the plasma temperature and thereby degrade the plasma performance. Much effort is being made by various groups to provide spectroscopic data for W in many charge states and over wide spectral regions [1–3]. Unfortunately, for plasma diagnostic purposes, there is very little spectroscopic data for tungsten in the charge states between W^{6+} and W^{28+}.

The atomic structure for many of the ions in this region is very complicated, and in some cases it is not even possible to easily establish the electronic ground configuration. For example in W^{7+} it is not clear whether $4f^{13}5s^25p^6\ {}^2F_{7/2}$ or $4f^{14}5s^25p^5\ {}^2P_{3/2}$ is the lowest level of the ground state—a confusion that arises from the fact that the $4f$ and $5p$ orbitals have almost the same binding energy in this ion.

The W^{27+} ion has a relatively simple ^2F ground state and an $M1$ line connecting the lowest $^2F_{5/2}$ with the $^2F_{7/2}$ has already been the subject of some theoretical investigations [4–6]. This fine-structure interval is also given in the comprehensive review of available tungsten data by Kramida and Shira [7]; however, as will be discussed below, there are reasons to doubt the value quoted in Ref. [7]. This $M1$ line is the subject of the work reported here. An $M1$ forbidden line is also expected to connect the levels in the ground-state doublet, whether ^2F or ^2P, in W^{7+}. Accurate measurements of the wavelengths of these lines would give precise values for the ground-state fine structures in these ions. These fine structures would in turn be useful for establishing more reliable theoretical models for these and the more complex close by ions. There are also some previously observed lines from W^{13+} in the soft-x-ray region [8]. Similar to the above, accurate wavelength measurements can help to establish good theoretical models for tungsten ions with charge states around 13+. It is clear that one of the most versatile light sources for studying tungsten spectroscopy, in all of its charge states, is the electron beam ion trap (EBIT); in fact, the data referenced in Refs. [1–3] are all from EBIT facilities. EBITs have been in existence now for over 25 years with the first such device being developed at the Lawrence Livermore Laboratory [9]. Most EBITs use superconducting magnets to provide the field for compressing the electron beam; however, room-temperature EBITs also have a fairly long history [10], where less compression of the electron beam is required.

The work presented here focuses on a visible $M1$ ground-state transition between the $4f\ {}^2F_{5/2}$ and $4f\ {}^2F_{7/2}$ levels in W^{27+}. The spectra were recorded using the recently developed Shanghai permanent magnet EBIT (SH-PermEBIT) [11]. We also carried out a theoretical study of the ground-state fine structure of Ag-like ions, including W^{27+}, using a revised version of the GRASP2K codes [12]. The fine structure defining the wavelength for this transition has been measured by soft-x-ray spectroscopy [13] and this energy is reported in the compilation by Karamida and Shirai [7] as $33\,000 \pm 800\ \mathrm{cm}^{-1}$; this leads to a wavelength of 3030 ± 75 Å. Recent calculations by Ivanova *et al.* [4] and Ding *et al.* [5] give wavelengths for this transition at 3147.8 and 3430.4 Å, disagreements large enough to promote further investigation.

The importance of visible forbidden transitions from tungsten ions in ITER plasma diagnostics was discussed in a recent paper by Skinner [14]. Although this $M1$ line is just outside the visible region of interest reported in Ref. [14], it is important to understand the atomic structure here as a guideline when working with the more difficult W ions in the range of charge states between 7+ and 27+.

II. EXPERIMENTAL METHODS

We have developed a room-temperature EBIT capable of operating in the range of electron beam energies between 60 and 5000 eV [11]. We can therefore create W ions in charge states from very low, two or three times ionized, up to almost 50 times ionized. The design and operating conditions of the SH-PermEBIT are discussed in some detail in Refs. [11,15].

*Corresponding author: rhutton@fudan.edu.cn

†Corresponding author: zouym@fudan.edu.cn

 ©2012 American Physical Society

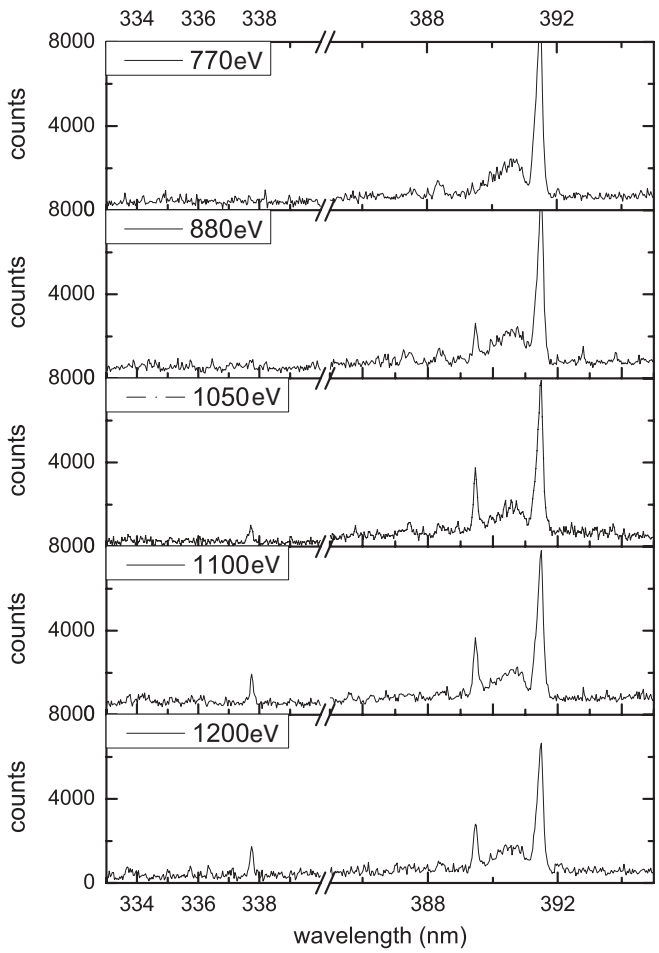

FIG. 1. Visible spectra taken at the SH-Perm EBIT, at the electron beam energies of 770, 880, 1050, 1100, and 1200 eV with a beam current of 5.5 mA, while injecting $W(CO)_6$. The W^{27+} $^2F_{5/2} \rightarrow {}^2F_{7/2}M1$ line can be seen to appear between 337 and 338 nm. The line between 389 and 390 nm is the W^{26+} $^3H_5 \rightarrow {}^3H_4$ $M1$ line 389.41 nm recently identified in Ref. [21], and the line at 391.44 nm is the $N_2{}^+$ line, from the residual gas inside the EBIT trap.

As shown in Ref. [11] we have operated our low-energy EBIT at 60 eV with an electron beam current of 2.4 mA. The EBIT plasma can be viewed by a number of spectrometers: one is a so-called flat field spectrometer covering the wavelength of 5–30 nm [16] and the other is a Czerny-Turner spectrometer from Andor, which covers the range of 200–800 nm. These two spectrometers and the EBIT form a tabletop setup for studies of highly charged ion spectroscopy.

In this work we studied the visible $M1$ ground-state transition between the $4f$ $^2F_{5/2}$ and $4f$ $^2F_{7/2}$ levels in W^{27+}. The tungsten ions for the study presented here were obtained by injecting $W(CO)_6$. $W(CO)_6$ is a volatile compound which has a high enough vapor pressure at room temperature for injection into the EBIT. Once the $W(CO)_6$ molecules enter the region of the electron beam they are quickly destroyed and the W atoms are ionized in further collisions with beam electrons. The final W charge state distribution depends on a number of parameters, for example, the electron beam energy, current density, injection rate, and also on a balance among the processes of ionization, recombination, charge exchange, etc. Once the ions are formed, they are consequently trapped in the radial direction by the space charge of the electron beam and the magnetic field of the EBIT, and longitudinally by voltages applied to the EBIT drift tubes (trap depth) [11]. Finally the trapped ions occupy a region in space at the center of the EBIT which is around 2 cm long and 0.1 mm (FWHM) in diameter. Photons emitted by the ions are focused by a quartz lens, positioned outside the EBIT, onto the entrance slit of an Andor SR-303i spectrometer. The grating we used had 1200 l/mm and the photons were imaged onto and detected by an Andor Newton CCD camera.

In the experiment, measurements were done at electron beam energies 770, 880, 1050, 1100, and 1200 eV, with a beam current of 5.5 mA, and trap depth of 200 eV. The spectral recording time for each spectrum was 3 h. The recorded spectra are shown in Fig. 1.

The spectral range focused on in this study is 330–400 nm. The spectrometer was calibrated mostly by an external Hg lamp, with the exception of a line from $N_2{}^+$ at 391.44 nm, which is from the residual gas inside the EBIT trap. All the calibration lines are listed in Table I. By least-squares fitting to the five calibration lines we determined the uncertainty in the measured W^{27+} line to be 0.26 Å.

III. DESCRIPTION OF THE CALCULATION

We use the multiconfiguration Dirac-Fock method, which is based on an expansion of the atomic state function in a linear combination of

$$\Psi(\gamma J) = \sum_{i=1}^{M} \phi(\gamma_i J), \tag{1}$$

where the configuration state functions (CSFs) $\phi(\gamma_i J)$ are formed as a linear combination of products of spin orbitals for each electron. The CSFs are generated as all possible combinations of orbitals in an active set (AS), according to certain constraints, to form a restricted active space (RAS) of CSFs. The first step is to include only the main configuration, in our case $1s^2 2s^2 2p^6 3s^2 3p^6 3d^{10} 4s^2 4p^6 4d^{10} 4f$ with $J = 5/2$ and $7/2$ in a single configuration approach—in the future labeled Dirac-Fock (DF). The orbitals are then optimized in a Dirac-Coulomb model [12]. Corrections to this arise from two different sources: (1) Breit and QED corrections [19], which can be included in a final configuration interaction calculation,

TABLE I. The five calibration lines used in this work, including four lines from a Hg lamp [17] with standard error about 0.0001 nm and also an $N_2{}^+$ line [18].

Calibration lines	Hg I($^3P_2$-$^3S_1$)	Hg I($^3P_2$-$^3D_3$)	Hg I($^3P_2$-$^3D_2$)	Hg I($^3P_2$-$^1D_2$)	$N_2{}^+$
Wavelength (nm)	334.148	365.016	365.484	366.328	391.440

after the optimization of the orbitals; and (2) correlation, which is treated by the multiconfiguration approach in Eq. (1).

In this study we are aiming for single-line spectroscopy, that is, we would like to identify a species by only observing one transition, and therefore it is essential to reach very high accuracy. For a system like W^{27+}, with only one electron outside closed core subshells, we can classify the correlation according to (a) core-valence (CV) correlation, i.e., correlation between the outer $4f$ electron and an electron in one of the core subshells; and (b) core-core (CC) correlation, i.e., correlation within the core subshells—either as "intra-CC" within one core subshell or "inter-CC" between two core subshells.

The CV correlation is in our model introduced by including CSFs in expansion (1) generated by allowing one excitation from a core subshell. For example, CV with a $4d$ electron is included via CSFs of the form $1s^22s^22p^63s^23p^63d^{10}4s^24p^64d^9nln'l'$ or with a $3d$ electron included via $1s^22s^22p^63s^23p^63d^94s^24p^64d^{10}nln'l'$ CSFs. The intra-CC in, e.g., $4p$ can be included via $1s^22s^22p^63s^23p^63d^{10}4s^24p^44d^{10}nln'l'n''l''$ CSFs (such a model also includes CV with $4p$). Finally, inter-CC, between, e.g., $3p$ and $3d$, can be included via CSFs of the form $1s^22s^22p^63s^23p^53d^94s^24p^64d^{10}nln'l'n''l''$, where CV with $3p$ and $3d$ is also included.

As always when using methods such as the multiconfiguration Dirac-Hartree-Fock method, we start the analysis by performing a DF and then adding Breit and QED corrections (see the first three rows in Table III). From this it is clear that the Breit correction decreases the fine structure by more than 1500 cm^{-1}, while QED increases it by around 20 cm^{-1}.

To explore the importance of different correlation contributions we start with a, what we will refer to as, separate approach for core-valence correlation (SCV). In this model we investigate the effect on the fine structure by including correlation with one core subshell at the time. The accumulative effect of these, i.e., the sum of all the corrections to the DF fine structure from SCV calculations, is then also a first estimate of the fine structure including CV.

TABLE II. The SCV model. Study of the different core-valence contributions to the energy split, relative to the value from Dirac-Fock + Breit and QED corrections. The total value is the sum of all contributions plus the DF-Breit-QED energy. Values are given in cm^{-1}.

	Active space no.			
Core subshell	AS1	AS2	AS3	AS4
$1s$	1	1	1	1
$2s$	4	5	6	6
$2p$	11	14	15	15
$3s$	13	17	18	18
$3p$	59	79	83	83
$3d$	150	181	187	189
$4s$	14	12	17	16
$4p$	68	48	51	50
$4d$	−7	−9	−6	−5
Sum	313	348	372	373
Total	29 574	29 609	29 633	29 634

The different core-valence correlation contributions resulting from this SCV model are presented in Table II. It is interesting that the contribution to the fine structure is important very deep in the core—as a matter of fact, over 50% of the increase of the fine structure due to CV, which is about 340 cm^{-1}, is due to correlation with $3d$. This knowledge is especially important since CV often is included only for the outermost core subshell. In this case that would be $4d$, which in fact gives a negative contribution to the fine structure, while CV actually seems to yield a quite large positive contribution. Note that the energies presented in Table III are relative to DF + Breit + QED.

Based on these results, armed with the knowledge that basically all CV correlation is important, we then perform a full-CV (FCV) calculation, where such correlation is included for all subshells simultaneously. In this model we increase our active set of orbitals in a systematic approach. Now the nl, $n'l'$, and $n''l''$ in our examples above belong to the following active sets:

$$\mathrm{AS1} = 4f + \{5s,5p,5d,5f,5g\},$$
$$\mathrm{AS2} = AS1 + \{6s,6p,6d,6f,6g,6h\},$$
$$\mathrm{AS3} = \mathrm{AS2} + \{7s,7p,7d,7f,7g,7h,7i\},$$
$$\mathrm{AS4} = \mathrm{AS3} + \{8s,8p,8d,8f,8g,8h,8i\}.$$

From exploratory calculations we found that symmetries up to and including $l = 6$ gave significant contributions to the fine structure. In the SCV and SCC calculations we did, however, only include symmetries up to and including $l = 4$, since these are only meant to be estimates of the size of CV and CC effects.

This is the most sophisticated model we present in this work—note, however, that it excludes all forms of core-core correlation. When including core-core correlation the size of the active space increases rapidly with the active set and therefore convergence is hard to achieve. To investigate the

TABLE III. Dirac-Fock energies with Breit, self-energy, and vacuum-polarization corrections (QED), followed by a comparison between our FCV calculation, our experiment, and other performed calculations. Note that the intra-CC contribution is an estimation of the actual value from the SCC model.

Source		Energy (cm^{-1})
DF		30 750
DF + Breit		29 239
DF + Breit + QED		29 261
FCV	AS1	29 451
	AS2	29 533
	AS3	29 574
	AS4	29 593
	AS5	29 603
	AS5 + intra-CC	29 570
Experiment (this work)		29 599.81 ± 2.28
Other theoretical work		
Safronova and Safronova [6] (RMBPT)		29 550
Ivanova [4] (RPTMP)		31 769
Ding *et al.* [5] (MCDF)		29 151

TABLE IV. The SCC model as compared to SCV, which gives an estimated value of the core-core correlation effects. Values are given in cm^{-1}.

	Active set no.			
Core subshell	AS1	AS2	AS3	AS4
$1s$	3	3	3	3
$2s$	− 3	− 3	− 3	− 2
$2p$	− 8	− 10	− 11	− 11
$3s$	− 2	− 4	− 4	− 4
$3p$	49	− 7	− 3	− 4
$3d$	− 42	− 14	− 13	− 14
$4s$	− 2	3	0	1
$4p$	14	9	2	2
$4d$	− 98	11	− 5	− 4
Sum	− 89	− 12	− 34	− 33

different CC effects, we therefore carry out a calculation applying a similar approach as for the SCV, that is, including core-core correlation with only one subshell at the time. The different SCC contributions are then compared to the corresponding SCV values. This gives us an approximated value for the size of the different core-core effects of about -33 cm^{-1} (see Table IV). The results show a surprisingly large contribution from some deep subshells ($2p$ and $3d$). An expansion of the FCV model would then preferably include CC correlation with, at least, these two orbitals. This is going to be investigated further elsewhere. As for now we give an estimated value including intra-CC as a correction to FCV AS5 (see Table III). In Fig. 2 we show the convergence of the FCV, as well as the SCC and SCV methods.

IV. RESULTS AND DISCUSSION

We use the recently identified W^{26+} line, at 389.41 nm, by Komatsu *et al.* [20] as a check on our $W(CO)_6$ injection. This line can be seen in Fig. 1 along with the W^{27+} $M1$ line, which is the subject of this work. The ionization potential of W^{25+} leading to the W^{26+} line is 784 eV and the ionization potential of W^{26+} is 833 eV [7], and hence we expect the W^{26+} line to appear at lower electron beam energy compared to the W^{27+} line. This is shown in Fig. 1, which shows how the spectrum develops as a function of the electron beam energy. Using the same line of argument we would not expect to see any line from W^{28+} for about 50 eV after the onset of the W^{27+} line. We would also not expect any W^{28+} line in this region of the spectrum, as W^{28+} has a closed $4d$ shell and hence no ground-state fine structure. There are a number of theoretical values for this transition, including our own obtained using the GRASP code. Our experimental wavelength of 3377.43 ± 0.26 Å (3378.43 Å vacuum wavelength) is compared to the calculated wavelengths in Table III.

It appears there is some confusion as to whether there existed an experimentally determined fine-structure energy for the ground state of W^{27+}. The first spectrum of W^{27+} was published by Isler *et al.* [21] in 1977 where they reported six lines that they believed to be from this ion at 47.94, 48.72, 49.37, 50.87, 51.49, and 52.35 Å. In 1981, Kaufman and Sugar published a paper [13] where they identified all the lines from Ref. [21] except the 47.94 Å line. From their work they could determine the fine-structure splitting of the ground state to 31 800 cm^{-1}. In that paper they studied Ag-like ions along the isoelectronic sequence Ce^{11+} to Ho^{20+} and W^{27+}, where the latter spectrum was referred to as "private communication R. C. Isler (1979)." In a later paper from 1993 by the same authors [22], they cast doubt on their earlier results for W^{27+} in Ref. [13], and they no longer claim that the ground-state fine-structure splitting had been experimentally determined. In that paper they also point out that the 47.94 Å line in Ref. [21] could not be a W line since the intensity of this line does not vary with the amount of tungsten injected into the plasma.

In the tungsten compilation by Kramida and Shirai [7] an experimentally determined fine-structure energy of 33 000 ± 800 cm^{-1} for the ground state is given. This is based on

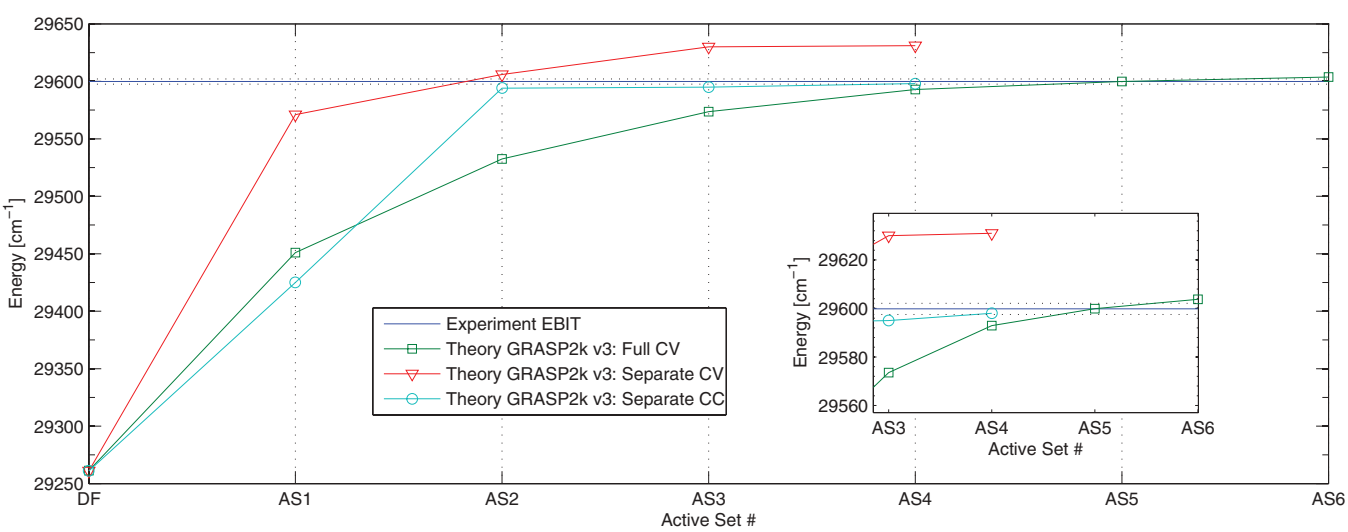

FIG. 2. (Color online) Convergence plot of the different approaches where FCV is the most sophisticated. SCV and SCC serve merely to show different CC and CV effects.

the identification of the 47.94 Å line from Ref. [21] and by making a nonrelativistic calculation using the COWAN code [23] to determine the fine-structure splitting of the ground state. We find this identification very puzzling for two reasons. First, because Sugar and Kaufmann [22] argue that the 47.94 Å line was not from tungsten and second, because large-scale relativistic calculations do not predict the fine-structure splitting to be around 33 000 cm^{-1} but 29 500 cm^{-1}.

V. CONCLUSION

It would appear from the comparison between our measured and calculated wavelengths for the W^{27+} $M1$ transition, and from the above discussion, that the fine-structure energy given in Ref. [7] is in error and should be revised. Also, it would be useful if other ions in the Ag I isoelectronic sequence could be studied to confirm our findings.

ACKNOWLEDGMENTS

This work was supported by the Chinese National Magnetic Confinement Fusion Science Program No. 2009GB106001, the National Natural Science Foundation of China No. 11074049, and by Shanghai Leading Academic Discipline Project No. B107. J.G. and T.B. gratefully acknowledge support from Swedish Science Foundation (Vetenskapsrådet).

[1] C. Biederman, R. Radtke, R. Seidel, and T. Pütterich, Phys. Scr., T **134**, 014026 (2009).
[2] Y. Ralchenko, I. N. Draganić, D. Osin, J. D. Gillaspy, and J. Reader, Phys. Rev. A **83**, 032517 (2011).
[3] J. Clementsson, P. Beiersdorfer, G. V. Brown, M. F. Gu, H. Lundberg, Y. Podpaly, and E. Träbert, Can. J. Phys. **89**, 571 (2011).
[4] E. P. Ivanova, At. Data Nucl. Data Tables **97**, 1 (2011).
[5] X. B. Ding, F. Koike, I. Murakami, D. Kato, Hiroyuki A. Sakaue, C. Z. Dong, N. Nakamura, A. Komatsu, and J. Sakoda, J. Phys. B **44**, 145004 (2011).
[6] U. I. Safranova and A. S. Safranova, J. Phys. B **43**, 074026 (2010).
[7] A. Kramida and T. Shirai, At. Data Nucl. Data Tables **95**, 305 (2009).
[8] R. Hutton, Y. Zou, J. Reyna Almandos, C. Biedermann, R. Radtke, A. Greier, and R. Neu, Nucl. Instrum. Methods Phys. Res. B **205**, 114 (2003).
[9] M. A. Levine, R. E. Marrs, J. R. Henderson, D. A. Knapp, and M. B. Schneider, Phys. Scr., T **22**, 157 (1988).
[10] V. P. Ovsyannikov and G. Zschornack, J. Instrum. **5**, C11002 (2010).
[11] J. Xiao, Z. Fei, Y. Yang, X. Jin, D. Lu, Y. Shen, L. Liljeby, R. Hutton, and Y. Zou, Rev. Sci. Instrum. **83**, 013303 (2012).
[12] P. Jönsson, X. He, C. F. Fischer, and I. P. Grant, Comput. Phys. Commun. **177**, 597 (2007).
[13] J. Sugar and V. Kaufman, Phys. Scr. **24**, 742 (1981).
[14] C. H. Skinner, Can. J. Phys. **86**, 285 (2008).
[15] X. L. Jin, Z. Fei, J. Xiao, D. Lu, R. Hutton, and Y. Zou, Physics of Plasmas **19**, 073505 (2012).
[16] Y. Yang, Z. Shi, Z. Fei, X. Jin, J. Xiao, R. Hutton, and Y. Zou, Phys. Scr., T **144**, 014064 (2011).
[17] C. J. Sansonetti, M. L. Salit, and J. Reader, Appl. Opt. **35**, 1 (1996).
[18] C. P. Lungu, M. Futsuhara, O. Takai, M. Braic, and G. Musa, Vacuum **51**, 635 (1998).
[19] I. P. Grant, *Relativistic Quantum Theory of Atoms and Molecules* (Springer, New York, 2007).
[20] A. Komatsu, J. Sakoda, N. Nakamura, H. A. Sakaue, X.-B. Ding, D. Kato, I. Murakami, and F. Koike, Phys. Scr., T **144**, 014012 (2011).
[21] R. C. Isler, I. V. Neidigh, and R. D. Cowan, Phys. Lett. A **63**, 295 (1977).
[22] J. Sugar, V. Kaufman, and W. L. Rowan, J. Opt. Soc. Am. B **10**, 1321 (1993).
[23] R. D. Cowan, *Theory of Atomic Spectra* (University of California Press, Berkeley, 1981).